Observation of Quantized Exciton Energies in Monolayer WSe_2 under a Strong Magnetic Field

Tianmeng Wang,[1,‡] Zhipeng Li,[1,‡] Zhengguang Lu,[2,3,‡] Yunmei Li,[4,‡] Shengnan Miao,[1] Zhen Lian,[1] Yuze Meng,[1] Mark Blei,[5] Takashi Taniguchi,[6] Kenji Watanabe,[6] Sefaattin Tongay,[5] Wang Yao,[7] Dmitry Smirnov,[2] Chuanwei Zhang,[4,*] and Su-Fei Shi[1,8,†]

[1]*Department of Chemical and Biological Engineering, Rensselaer Polytechnic Institute, Troy, New York 12180, USA*
[2]*National High Magnetic Field Lab, Tallahassee, Florida 32310, USA*
[3]*Department of Physics, Florida State University, Tallahassee, Florida 32306, USA*
[4]*Department of Physics, The University of Texas at Dallas, Richardson, Texas 75080, USA*
[5]*National Institute for Materials Science, 1-1 Namiki, Tsukuba 305-0044, Japan*
[6]*School for Engineering of Matter, Transport and Energy, Arizona State University, Tempe, Arizona 85287, USA*
[7]*Department of Physics and Center of Theoretical and Computational Physics, University of Hong Kong, Hong Kong, China*
[8]*Department of Electrical, Computer & Systems Engineering, Rensselaer Polytechnic Institute, Troy, New York 12180, USA*

(Received 22 October 2019; revised manuscript received 11 March 2020; accepted 25 March 2020; published 30 April 2020)

Quantized energy levels are one of the hallmarks of quantum mechanics at the atomic level. The manifestation of quantization in macroscopic physical systems has showcased important quantum phenomena, such as quantized conductance in (fractional) quantum Hall effects and quantized vortices in superconductors. Here we report the first experimental observation of quantized exciton energies in a macroscopic system with strong Coulomb interaction, monolayer WSe_2 crystal under a strong magnetic field. Employing helicity-resolved magnetoreflectance spectroscopy, we observe a striking ladder of plateaus as a function of the gate voltage for both exciton resonance in one valley and exciton-polariton branch in the opposite valley, thanks to the inter-Landau levels transitions governed by unique valley-selective selection rules. The observed quantized excitation energy level spacing sensitively depends on the doping level, indicating strong many-body effects. Our work will inspire the study of intriguing quantum phenomena originating from the interplay between Landau levels and many-body interactions in two-dimension monolayer crystals.

DOI: 10.1103/PhysRevX.10.021024

Subject Areas: Condensed Matter Physics, Nanophysics, Optics

I. INTRODUCTION

Quantized energy is a fundamental property for physical systems at the atomic scale, such as the spectra of hydrogen atoms and single atom trapped in an optical tweezer [1,2]. In some macroscopic quantum systems, quantized physical quantities, usually originating from topology, defect, or interaction, have also been observed, and well-known examples include quantized vortices in superfluids and superconductors [3–5], quantum Hall effects (QHEs) [6–9], etc. Among them, quantized Hall conductance is one of the most striking phenomena in condensed matter physics. In two-dimension (2D) electron gases, the out-of-plane magnetic field forms quantized Landau levels (LLs) for carries [10,11]. With low magnetic fields, the LLs lead to quantum oscillations such as the Shubnikov–de Haas (SdH) oscillations, while quantized Hall conductance emerges with a strong magnetic field due to the topological band of the highly degenerate LLs [12–17]. Strong many-body interaction can lead to further fractionalization of quantized Hall conductance [18,19].

Monolayer transition metal dichalcogenides (TMDCs) offer an intrinsic 2D semiconductor system for the study

*Corresponding author.
Chuanwei.Zhang@utdallas.edu
†Corresponding author.
shis2@rpi.edu
‡These authors contributed equally to this work.

of quantum physics with a magnetic field, where optical signature plays a major role in exploring material properties. In particular, the optically excited electron-hole pair forms an exciton with a large exciton binding energy of hundreds of meV [20–23] because of the enhanced Coulomb interaction in 2D due to reduced screening. In monolayer TMDCs, the nontrivial Berry phase [24–28] and strong spin-orbital coupling [13] lead to a set of valley- and spin-polarized LLs with unique transition rules [10,11]. The coexistence of such LLs and strongly bound exciton [13–17] raises an intriguing question: Will the quantized LLs work as a series of tunable band gaps and host excitons with quantized energies? Although the valley- and spin-polarized LLs have been demonstrated in the reflectance spectra of highly n-doped WSe_2, the much-reduced binding energy of the exciton renders the inter-LL transition similar to the band edge transition of conventional semiconductors [29]. A recent work on $MoSe_2$ explores the LLs' effects in the low p-doping region, in which the exciton binding energy is still significant. However, only Shubnikov–de Haas-type of oscillation was observed in the optical reflectance spectra [30].

In this work, we report the first experimental observation of quantized exciton energies in a macroscopic system with strong Coulomb interaction. We achieve this through the helicity-resolved magnetoreflectance spectra of a high-quality monolayer WSe_2 device under an out-of-plane magnetic field up to 31 T, and the Landau quantization of the exciton energy clearly occurs in the lightly p-doping region. Here the optical signature of the inter-LL transition is tuned by the gate voltage that controls the Fermi energy. Because of the valley-Zeeman shift, at the finite shift of Fermi energy, it could be realized that only one valley of TMDC is doped while the opposite valley remains charge neutral. As a result, the magnetoreflectance spectrum is dominated by the exciton resonance in one valley and the exciton-polaron resonance in the opposite valley. Here the exciton-polaron branch arises when the Fermi energy is non-negligible compared with the trion binding energy (20–30 meV [31–35]). Therefore, instead of forming the trion with a free carrier from the opposite valley, the exciton interacts with the whole Fermi sea of the opposite valley [30,36,37].

We also observed the signature of valley-polarized LLs from the highly electron-doping regime [29], which shows distinctively different behavior compared with the Landau quantization of the exciton in the hole-doping regime. In the slight hole-doping regime, the exciton resonance energies start to exhibit quantized plateaus with abrupt jumps when the Fermi energy crosses different LLs, which is also significantly different from the SdH-like resonance energy shift previously observed in $MoSe_2$ [30]. The exciton-polaron branch exhibits a correlated intensity oscillation, in agreement with theoretical prediction [36,37]. In the heavily hole-doping regime, even the exciton-polaron branch exhibits quantized resonance plateaus when the Fermi energy is further tuned below both valence bands. Further, the quantitative analysis reveals that the plateau spacing for the neighboring inter-LL transition for hole-doped WSe_2 is only about half of the value for electron-doped WSe_2, suggesting different excitonic physics that leads to the Landau quantization of the exciton energy in the p-doped regime compared with the LL signatures in the highly n-doped regime. The extremely high-quality monolayer WSe_2 device in the presence of the strong magnetic field thus provides an exciting platform for investigating the interplay of LLs and many-body interactions in 2D monolayer crystals with rich spin and valley physics.

II. OPTICAL REFLECTANCE SPECTRA

The BN encapsulated monolayer WSe_2 device is schematically shown in Fig. 1(a), and the fabrication details can be found in our previous work [38–40]. Since the reflectance spectrum of the monolayer WSe_2 at the top-gate voltage of −4 V is rather flat and has no resonance feature, we use it as the reference and obtain the reflectance spectra of monolayer WSe_2 by subtracting the reflectance spectra at a given gate voltage from the reference, i.e., by $\Delta R = R(V_g) - R(-4\ \mathrm{V})$. The optical reflectance spectra at 4.2 K are plotted as a function of the top-gate voltage in Fig. 1(c). The high quality of the reflectance spectra is evidenced by the well-resolved resonance peaks of the intervalley trion (X_2^-) and intravalley trion (X_1^-), as well as the reflectance resonance corresponding to the $2s$ state of the A exciton (X_0^{2s}) [41–46]. The clear optical signature of different excitonic resonances also divides Fig. 1(c) into four different doping regimes: (I) charge-neutral region, in which $1s$ (X_0) and $2s$ (X_0^{2s}) resonances of the A exciton are most pronounced; (II) hole-doped region, which is marked by the onset of the positive trion (X^+); (III) electron-doped region, which is marked by the onset of the negative trions resonance (X_1^-, X_2^-); (IV) heavily electron-doped region, which is signaled by the onset of the exciton-plasma mode (X'^-) [47].

The strong spin-orbit coupling in TMDCs generates a large splitting of the valence band (∼300–500 meV) and a sizable splitting of the conduction bands (∼20–40 meV) at the K and K' valley [48,49], and the resulted band structure for monolayer WSe_2 is schematically shown in Fig. 1(b). The different spin configurations locked with K and K' valleys result in the valley degree of freedom, and the exciton can be selectively generated in either K or K' valley using left- or right-circularly polarized light. As the reflectance spectra reflect the coherent absorption progress for monolayer WSe_2 [50,51], the helicity-resolved reflectance spectroscopy, which utilizes the light with certain helicity as the excitation and detects the reflected light of the same helicity, can directly probe the information of each valley specifically. Meanwhile, the application of the out-of-plane magnetic field has two major effects on the

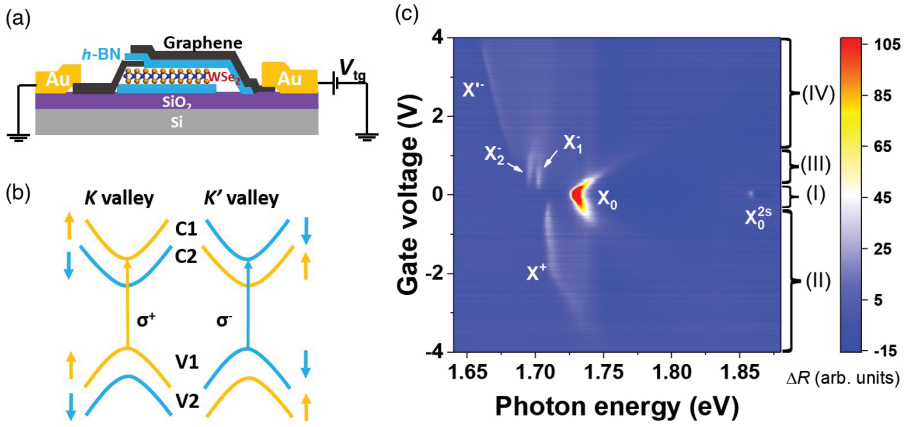

FIG. 1. Optical reflectance spectra of the top-gated monolayer WSe_2 device. (a) Schematic of the BN (blue) encapsulated monolayer WSe_2 device, contacted and top gated by few-layer graphene flakes (black). (b) Schematic of the band structure of monolayer WSe_2 at K and K' valleys, and the exciton can be selectively excited by the right-circularly polarized (σ^+) or left-circularly polarized (σ^-) light. Note that the spin-orbit coupling induced band splittings in the conduction and valence bands are not drawn to their actual scale. (c) The color plot of the optical reflectance spectra as a function of the top-gate voltage. The reflectance spectra were obtained by subtracting the reference reflectance spectra at the gate voltage of -4 V as the background, and the color represents the reflectance intensity difference. X_0, X_0^{2s}, X^+, X_1^-, X_2^-, and X'^- correspond to the absorption resonance at the A exciton, $2s$ state of A exciton, the positive trion, intervalley trion, intravalley trion, and the emerging plasmon polaron mode, respectively.

electronic structure. First, the opposite Zeeman splitting of the K and K' valleys lifts the energy degeneracy of the two valleys. Second, spin- and valley-polarized LLs start to develop in both valleys [Fig. 2(c)].

We measure the helicity-resolved reflectance spectra of each valley in the presence of the out-of-plane magnetic field, and the data for the magnetic field of 25 T are shown in Fig. 2(a) (K valley, σ^+ excitation, and σ^+ detection) and Fig. 2(b) (K' valley, σ^- excitation, and σ^- detection). The reflectance spectra in Figs. 2(a) and 2(b) are distinctively different, especially in the lightly hole-doping regime (Fermi energy between μ_3 and μ_4 in Fig. 2). At K valley, the exciton resonance extends into the hole-doping region (region II) and becomes quantized resonances with an overall blueshift with increased doping. At K' valley, in contrast, the exciton resonance quickly disappears in the hole-doping region, while the exciton-polaron resonance undergoes a redshift, along with a periodic intensity oscillation [cf. the enlarged plot in Fig. 3(d)]. The exciton-polaron resonance becomes quantized resonance peaks when WSe_2 is highly hole doped [top-gate voltage < -2.10 V, corresponding to Fermi energy below μ_4 in Fig. 2(b)]. We show in the later discussion that the asymmetry between the K and K' valley is due to the lift of energy degeneracy of the two valleys by the magnetic field, and the position of the Fermi energy sensitively determines the nature of the exciton-electron interaction.

The differential reflectance spectra also exhibit a striking difference in the n-doping and p-doping regime. In the lightly n-doping region (gate voltage from 0.22 to 0.95 V, region III), we still observe two negative trions, similar to the scenario without the magnetic field. However, the PL

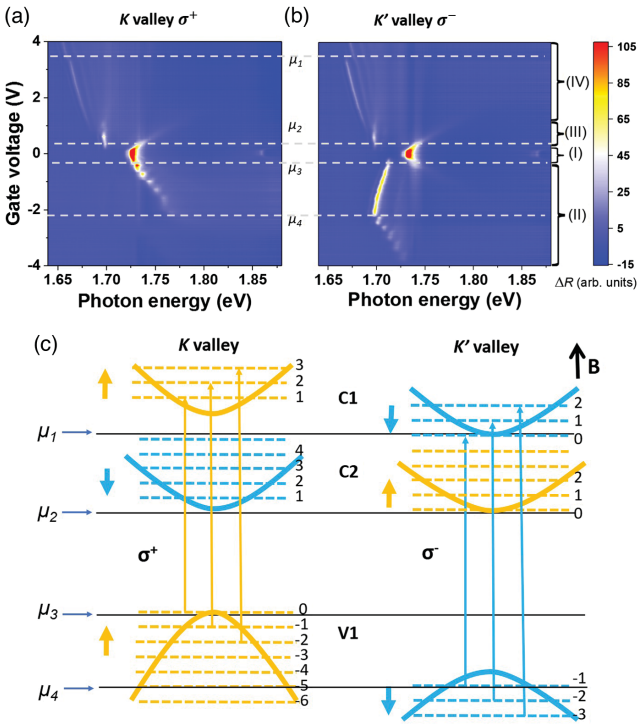

FIG. 2. Helicity-resolved optical magnetoreflectance spectra. (a),(b) Color plots of the helicity-resolved optical reflectance spectra for K and K' valleys, respectively, as a function of the top-gate voltage with the application of the out-of-plane magnetic field of 25 T. (c) The magnetic field lifts the degeneracy of the K and K' valley, and LLs form in the conduction and valence band. The arrows indicate the allowed inter-LL transitions in the K and K' valley. Fermi energies of μ_1, μ_2, μ_3, and μ_4 correspond to different doping levels controlled by the top-gate voltage.

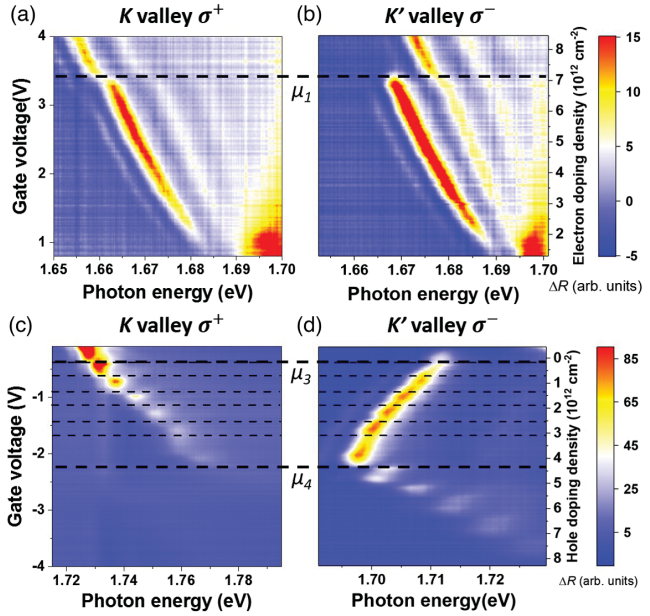

FIG. 3. Magnetoreflectance spectra modified by inter-LL transitions. (a),(b) Enlarged color plots of the helicity-resolved optical reflectance spectra for K (a) and K' (b) valleys in Figs. 2(a) and 2(b), in the highly n-doped region. (c),(d) Enlarged color plots of Figs. 2(a) and 2(b) in the p-doped region.

from the two negative trions are not equal in intensity at the presence of the out-of-plane magnetic field, with that of X_1^- (intervalley exciton) stronger in the K valley and X_2^- (intravalley exciton) stronger in the K' valley. This is due to the degeneracy lifted by the out-of-plane magnetic field, under which the lower conduction band (C2) in the K' valley is slightly below the C2 in the K valley [Fig. 2(c)]. As a result, the negative trion absorption from the K valley (with the electron and hole pair residing in the K valley) is mostly from the intervalley exciton X_1^-, while that from the K' valley is mostly from the intravalley exciton X_2^- (also see Supplemental Material, Sec. XII [52]).

As the gate voltage is increased to >0.95 V (region IV) in which X'^- emerges, we observe a set of Landau-fan-like patterns that are consistent with the previous report and were previously attributed to the inter-LL transition [15,17,29]. The correlation of the optical signature of LLs in the n-doping side with the onset of the exciton-plasma mode indicates the importance of many-body interaction to observe the LLs' effect in the reflectance spectra. In this work, we focus on the hole-doping regime (region II), where we observe either a set of discrete exciton resonances (K valley) or intensity oscillation of the exciton-polaron resonance (K' valley). Both will be shown later to be attributed to the LLs' formation. This apparent asymmetry between the n-doping and p-doping regions might arise from the unique band structure of monolayer WSe_2, in which the spin-orbit coupling induced splitting of the conduction bands dictates that the lower energy conduction band [C1 in Fig. 2(c)] has opposite spin compared to that of the valence band maximum (VBM). The bright exciton, therefore, has to be formed with the electron in the C2 band and hole in the V1 band [Fig. 2(c)]. While the p-doping immediately fills the VBM and directly affects the bright exciton formation through the phase filling effect, the initial n doping only fills the C1 band and does not affect the bright exciton formation, which involves C2 band. As a result, the LL effects in the n-doping region occur at high-doping density, which greatly reduces the Coulomb interaction and significantly modifies the excitonic physics. The coincidence of the onset of the Landau-fan feature in the n-doping region with the plasmon mode also suggests different excitonic physics, compared with the strongly bound exciton in the lightly p-doped regime. However, the exact microscopic mechanism needs to be investigated later, which is beyond the scope of this work.

In the n-doping region, the reflectance spectra modified by the inter-LL transition can be seen more clearly in Figs. 3(a) and 3(b), which are enlarged images from Figs. 2(a) and 2(b). These observations are similar to the previous report by Wang *et al.* [29] and can be quantitatively understood with the inter-LL transition, considering the set of LLs developed in the valence band and conduction band independently. It is worth noting that, similar to graphene, the nontrivial Berry phase in TMDCs dictates the existence of LL with index $n = 0$ [Fig. 2(c)]. Previous theory study [11] has shown that, in contrast to the selection rules of two-dimensional electron gas (2DEG) and graphene that requires $|n| = |n'| \pm 1$, where n and n' are the LL index, the inter-LL transition in TMDCs is governed by valley-selective selection rules [11,25,29]. Namely, the only allowed transitions are $-n \leftrightarrow n+1$ transition in K valley and $-(n+1) \leftrightarrow n$ in K' valley. These allowed transitions can be tuned by controlling the Fermi energy through doping. For example, as shown in Fig. 2(c), the $-1 \leftrightarrow 0$ transition in the K' valley will be blocked if the Fermi energy is increased to the C2 band, which corresponds to the termination of one of the Landau-fan-like resonances shown in the reflectance spectra, indicated by the dashed line in Fig. 3(b). Based on the previous report of the conduction band splitting of 40 meV [29], the correlation of the gate voltage to the Fermi energy shift in our device can be established.

In this work, we focus on the hole-doping region, in which the effect of LLs can be observed only in high-quality samples. We show in Figs. 3(c) and 3(d) the enhanced enlarged color plot of the hole-doped region in Figs. 2(a) and 2(b). The reflectance spectra could be understood with the consideration of both the Zeeman splitting effect and the LLs' formation for K and K' valleys ($B > 0$ here), shown schematically in Fig. 2(c). The intensity oscillation in the hole-doping side from the K' valley has been theoretically [36,37] investigated and attributed to the magnetic field dependence of the repulsive exciton-polaron, which is a quasiparticle of the exciton

interacting with the entire Fermi sea in the opposite valley. The simple picture of a trion, which consists of one exciton with one free electron or hole in the opposite valley, is only valid for small doping, or $E_F \ll E_T$, in which E_F is the Fermi energy associated with the doping and E_T is the binding energy of the trion. For the gate voltage of −0.19 to −2.10 V, corresponding to the Fermi energy between μ_3 and μ_4, the exciton in the K' valley interacts with the entire Fermi sea of the holes in the K valley, and the exciton-polaron undergoes a redshift along with intensity oscillation, as shown in Fig. 3(d). Recently, a helicity-resolved reflectance spectroscopy study of monolayer $MoSe_2$ has shown exciton-polaron intensity oscillation in the hole-doped high-quality monolayer $MoSe_2$ device [30]. We note that the exciton-polaron intensity oscillation in our monolayer WSe_2 device is much more pronounced, likely due to improved sample quality and stronger magnetic field applied.

When the Fermi energy is between μ_3 and μ_4, as free holes only exist in the K valley but not in the K' valley, no free holes are available in the K' valley to form the exciton-polaron with the excited exciton in the K valley. As a result, the optical reflectance spectra from the K valley [Fig. 3(c)] are dominated by the exciton resonances from the inter-LL transitions. We observed that the exciton resonance energy at zero doping is not a sensitive function of the magnetic field, only modified slightly by the valley-Zeeman shift, which is consistent with our numerical calculations that show the exciton binding energy not significantly affected by the magnetic field (see Figs. S4 and S8 in Supplemental Material [52]). Because the exciton binding energy is much larger than that of the LL spacing, a large number of LLs from the conduction and valence bands need to be taken into consideration to construct the exciton wave function in the numerical calculations. Quantized exciton resonances occur when the Fermi energy crosses each LL individually as the doping is increased, corresponding to the sequential filling of LL which is then not involved in the exciton wave function. Because of the large exciton binding energy and the number of LLs involved, the quantized exciton energy in this low-doping regime is not determined simply by the inter-LL transition spacings from the single-particle spectrum [15]. It is also interesting to note that, in the p-doped region, only one exciton resonance is visible at a fixed gate voltage in the reflectance spectra. In contrast, in the n-doped region, multiple excitonic resonances coexist in the reflectance spectra.

III. DISCUSSION

The quantized exciton energy at K valley [Fig. 3(c)] can be better visualized in Fig. 4(a), in which the exciton

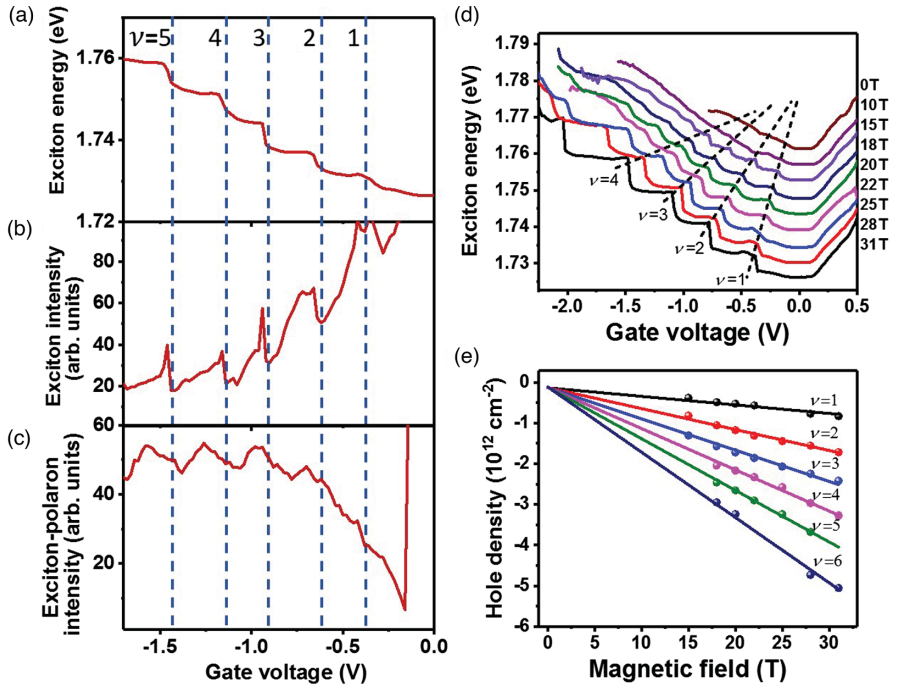

FIG. 4. Quantized exciton energy and spin- and valley-polarized LLs. (a) Under the out-of-plane magnetic field of 25 T, the reflectance spectra local maximum position was tracked as a function of the gate voltage. The exciton resonance energy as a function of the gate voltage for different LL filling factors exhibits a ladder of plateaus. (b) Integrated exciton differential reflectance intensity as a function of the gate voltage for different filling factors. (c) Integrated reflectance intensity for the exciton-polaron as a function of the gate voltage for different filling factors. (d) Exciton resonance energy as a function of the gate voltage for different magnetic field applied. The plateau feature starts to develop when the magnetic field exceeds 15 T. For each curve in different magnetic fields, we shift the energy of each curve by 4 meV for clarity. (e) The required hole density to completely fill the LL with the filling factor from 1 to 6.

resonance energy is plotted as a function of the gate voltage. It is evident that, with the sequential filling of the LLs in the valence band (filling factor ν noted) for increased p doping, the resonance energy exhibits a series of plateaus, each corresponding to the blocking of a low-energy LL in the formation of an exciton such that its energy increases by the LL spacing. This is in stark contrast to the previous report in monolayer $MoSe_2$, in which only a SdH-like oscillation of the resonance energy on top of a smooth blueshift background was observed. We attribute the plateaulike resonance energy shift to the improved sample quality that reduces the scattering and the larger magnetic field that increases the LL spacing. The combination of these two effects ensures that the LL is well resolved, similar to what is required to observe QHE instead of SdH oscillations in low-temperature transport measurements [14,15,53–55]. In fact, optical spectroscopy techniques have been employed to investigate the QHE of 2DEG. It was found that when the LL is completely filled, which corresponds to the onset of the new plateau of the quantum Hall conductance, the optical absorption is at its a minimum [55–57]. Interestingly, we find the integrated reflectance intensity also shows a sudden change at the gate voltage corresponding to the quantum jump of exciton resonance.

At the K' valley, for the gate voltage between -0.19 and -2.10 V at the magnetic field of 25 T, the integrated reflectance spectra intensity of the exciton-polaron resonance shows oscillation [Fig. 4(c)] concurrent with the discrete exciton resonance shift observed in the K valley [Fig. 4(a)]. In the highly p-doped region when the Fermi energy is tuned to below μ_4 (gate voltage < -2.10 V), the exciton-polaron branch turns into a set of quantized resonances as well. This is because the corresponding Fermi energy is below μ_4 [Fig. 2(c)] and starts to fill LL sequentially in the K' valley, similar to what occurs in the exciton branch (K valley) between the gate voltage -0.19 to -2.10 V. Therefore, the reflectance spectra in the K' valley is dominated by quantized exciton-polaron resonance, dressed by the whole Fermi sea from the K valley.

Both quantized resonances from the exciton (K valley) and exciton-polaron branch (K' valley) can be utilized to construct the corresponding Landau fans [Fig. 4(e) and Fig. S3 in Supplemental Material [52]]. The quantized resonance energy (K valley) as a function of the top-gate voltage for different magnetic field is plotted in Fig. 4(d), which shows that the series of plateaus of exciton resonances occur for magnetic field ≥ 15 T, and the onset gate voltage for each plateau clearly shifts [dashed line in Fig. 4(d)] as the magnetic field strength increases. Based on a simple capacitance model, the density of the carrier will increase as a function of the gate voltage as 2.15×10^{14} cm^{-2} V^{-1} (see capacitance model in Supplemental Material [52]). Therefore, the hole density for the onset of each resonance plateau as a function of the B field can be plotted as the Landau fan shown in Fig. 4(e). The degeneracy of each LL can be calculated as $N_\nu - N_{\nu-1} = feB/h$, in which N_ν is the density of holes needed to completely fill the LL level in the valence associated with inter-LL transition index ν, and f is degeneracy. We found that f is about 1 (1.26, 1.06, 1.01, 1.05, and 1.39 for inter-LL transition index $\nu = 1$, 2, 3, 4, 5, respectively; see Fig. S2 in Supplemental Material [52]), confirming that all the LLs from the K valley are spin and valley polarized. In the highly p-doped regime, we observe the second set of quantized excitonic resonance [Fig. 3(d), below μ_4], which we attribute to the inter-LL transition in the K' valley as the Fermi energy is tuned to be below μ_4. In this regime, as the Fermi energy crosses both K and K' valleys, the observation of the sequential inter-LL transition associated excitonic resonance involving filling the LL in the K valley as well, and we expect a degeneracy $f = 2$. However, the required density of holes as a function of the B field significantly deviates from a linear fit and calls for future investigation (see Fig. S2 in Supplemental Material [52]).

Strikingly, the energy spacing between neighboring Landau quantized excitonic resonances (Δ_{LL}) in the lightly p-doping region is significantly different from what can be extracted from the reflectance spectra in the highly n-doping region. In the highly n-doping regime, at the gate voltage of 3 V and B field of 25 T, Δ_{LL} is about 12 meV. In contrast, in the slight p-doping region, Δ_{LL} is approximately 5.5 meV at LL with the filling factor $\nu = 1$, only half the value of that in the n-doping regime. The striking difference of the LL effects between the n-doping region and the p-doping region might arise from the unique band structure of WSe_2, in which the lower conduction band hosts the dark exciton and the Fermi energy has to be tuned to the second conduction band to modulate the inter-LL transition, as we discussed previously. This is consistent with our observation of the LL effects on the reflectance spectra in the highly n-doped region. We also notice that the Landau-fan pattern in the n-doping region is associated with the onset of the plasmon mode, suggesting that LL effects are different from what is observed in the lightly p-doped region, which is due to Landau quantization of strongly bound excitons.

The difference of the LL spacing extracted from the n- and p-doping regions can be phenomenologically explained with the effective mass renormalization with finite doping [58,59], which in the lightly p-doped region (Fermi energy below μ_3 in Fig. 2) expresses the reduced mass of exciton as $m_r = m_{r0}(1 + 0.043 r_s)$ with $r_s = (1/\sqrt{\pi\sigma} a_B^*)$, where $m_{r0} = 0.2 m_0$ is the theoretical exciton reduced mass with no interaction, and m_0 is the free-electron mass. σ is the carrier density. The effective Bohr radius is defined as $a_B^* = \{(a_B \varepsilon)/[m_{h(e)}/m_0]\}$,where a_B is the Bohr radius, $m_{h(e)}$ is the carrier mass without mass renormalization, and ε is the dielectric constant of h-BN.

Δ_{LL} of 12 meV in the highly n-doped region (Fermi energy above μ_1 in Fig. 2) corresponds to the electron doping density of $\sigma = 7.0 \times 10^{12}$ cm^{-2}, and this high-doping density leads to an effective reduced mass of $m_r = 0.24m_0$, which is close to the expected value with no interaction ($0.2m_0$). In the lightly hole-doping region, the Δ_{LL} of 5.5 meV corresponds to the hole density of $\sigma = 0.6 \times 10^{12}$ cm^{-2}, which is more than one order of magnitude smaller than the n doping of 7.0×10^{12} cm^{-2}. This much smaller density of carriers results in a much enhanced Wigner-Seitz radius r_s and thus a much larger effective reduced mass of $m_r = 0.34m_0$. The increased effective reduced mass for exciton stems from the low-doping density at which the Landau quantization of exciton occurs in the p-doped monolayer WSe_2, suggesting different physics from the LL effects observed in the highly n-doped region, in which the Coulomb interaction is much reduced and excitons can be approximated as electron-hole pairs with negligible binding energy [31]. The strong Coulomb interaction of the tightly bound exciton might explain the unequal exciton energy between the neighboring filling factor of LLs, evidence of significant interaction due to many-body effects (see Fig. S7 in Supplemental Material [52]).

IV. SUMMARY

By pushing the limit of the sample quality and applying a strong magnetic field, we have observed quantized excitonic resonance from both the exciton and exciton-polaron branches from the magnetoreflectance spectra of a monolayer WSe_2 device. The nonequal spacing of the excitonic resonance in the presence of the valley- and spin-polarized LLs is a manifestation of strong many-body interactions in 2D, which will inspire the future development of a microscopic many-body interacting model for detailed and quantitative understanding.

ACKNOWLEDGMENTS

We thank Professor Fan Zhang, Professor Long Ju, and Dr. Chenhao Jin for helpful discussions. Z. Li and S.-F. S. acknowledge support from AFOSR through Grant No. FA9550-18-1-0312. T. W. and S.-F. S. acknowledge support from ACS PRF through Grant No. 59957-DNI10. Z. Lian and S.-F. S. acknowledge support from NYSTAR through Focus Center-NY–RPI Contract No. C150117. S. T. acknowledges support from NSF DMR-1552220, DMR-1838443, and CMMI-1933214. The device fabrication was supported by Micro and Nanofabrication Clean Room (MNCR) at Rensselaer Polytechnic Institute (RPI). K. W. and T. T. acknowledge support from the Elemental Strategy Initiative conducted by the MEXT, Japan, and the CREST (JPMJCR15F3), JST. Z. Lu. and D. S. acknowledge support from the U.S. Department of Energy (DE-FG02-07ER46451) for magnetophotoluminescence measurements performed at the National High Magnetic Field Laboratory, which is supported by National Science Foundation through NSF/DMR-1644779 and the State of Florida. Y. L. and C. Z. are supported by AFOSR (Grant No. FA9550-16-1-0387), NSF (Grant No. PHY-1806227), and ARO (Grant No. W911NF-17-1-0128). S.-F. S. also acknowledges the support from a Knowledge and Innovation Program seed grant from RPI and a Visiting Scientist Program grant from NHMFL.

[1] D. Weiss and M. Saffman, *Quantum Computing with Neutral Atoms*, Phys. Today **70**, No. 7, 44 (2017).
[2] N. Bohr, *On the Constitution of Atoms and Molecules*, Philos. Mag. J. Sci. **26**, 476 (1913).
[3] A. J. Leggett, *Quantum Liquids: Bose Condensation and Cooper Pairing in Condensed-Matter Systems* (Oxford University Press, Oxford, 2008).
[4] P. W. Anderson, *Considerations on the Flow of Superfluid Helium*, Rev. Mod. Phys. **38**, 298 (1966).
[5] B. T. Matthias, T. H. Geballe, and V. B. Compton, *Superconductivity*, Rev. Mod. Phys. **35**, 1 (1963).
[6] S. D. Sarma and A. Pinczuk, *Perspectives in Quantum Hall Effects: Novel Quantum Liquids in Low-Dimensional Semiconductor Structures* (Wiley, New York, 1997).
[7] K. v. Klitzing, G. Dorda, and M. Pepper, *New Method for High-Accuracy Determination of the Fine-Structure Constant Based on Quantized Hall Resistance*, Phys. Rev. Lett. **45**, 494 (1980).
[8] J. Wakabayashi and S. Kawaji, *Hall Effect in Silicon MOS Inversion Layers under Strong Magnetic Fields*, J. Phys. Soc. Japan **44**, 1839 (1978).
[9] T. Ando, Y. Matsumoto, and Y. Uemura, *Theory of Hall Effect in a Two-Dimensional Electron System*, J. Phys. Soc. Japan **39**, 279 (1975).
[10] A. Kormányos, P. Rakyta, and G. Burkard, *Landau Levels and Shubnikov-de Haas Oscillations in Monolayer Transition Metal Dichalcogenide Semiconductors*, New J. Phys. **17** (2015).
[11] R.-L. Chu, X. Li, S. Wu, Q. Niu, W. Yao, X. Xu, and C. Zhang, *Valley-Splitting and Valley-Dependent Inter-Landau-Level Optical Transitions in Monolayer* MoS_2 *Quantum Hall Systems*, Phys. Rev. B **90**, 045427 (2014).
[12] J. Avron, D. Osadchy, and R. Seiler, *A Topological Look at the Quantum Hall Effect*, Phys. Today **56**, No. 8, 38 (2003).
[13] B. Fallahazad, H. C. P. Movva, K. Kim, S. Larentis, T. Taniguchi, K. Watanabe, S. K. Banerjee, and E. Tutuc, *Shubnikov–de Haas Oscillations of High-Mobility Holes in Monolayer and Bilayer* WSe_2*: Landau Level Degeneracy, Effective Mass, and Negative Compressibility*, Phys. Rev. Lett. **116**, 086601 (2016).
[14] H. C. P. Movva, B. Fallahazad, K. Kim, S. Larentis, T. Taniguchi, K. Watanabe, S. K. Banerjee, and E. Tutuc, *Density-Dependent Quantum Hall States and Zeeman Splitting in Monolayer and Bilayer* WSe_2, Phys. Rev. Lett. **118**, 247701 (2017).

[15] R. Pisoni *et al.*, *Interactions and Magnetotransport through Spin-Valley Coupled Landau Levels in Monolayer* MoS_2, Phys. Rev. Lett. **121**, 247701 (2018).

[16] S. Larentis, H. C. P. Movva, B. Fallahazad, K. Kim, A. Behroozi, T. Taniguchi, K. Watanabe, S. K. Banerjee, and E. Tutuc, *Large Effective Mass and Interaction-Enhanced Zeeman Splitting of K-Valley Electrons in* $MoSe_2$, Phys. Rev. B **97**, 201407(R) (2018).

[17] M. V. Gustafsson, M. Yankowitz, C. Forsythe, D. Rhodes, K. Watanabe, T. Taniguchi, J. Hone, X. Zhu, and C. R. Dean, *Ambipolar Landau Levels and Strong Band-Selective Carrier Interactions in Monolayer* WSe_2, Nat. Mater. **17**, 411 (2018).

[18] L. Saminadayar, D. C. Glattli, Y. Jin, and B. Etienne, *Observation of the* $1/3$ *Fractionally Charged Laughlin Quasiparticle*, Phys. Rev. Lett. **79**, 2526 (1997).

[19] V. J. Goldman and B. Su, *Resonant Tunneling in the Quantum Hall Regime: Measurement of Fractional Charge*, Science **267**, 1010 (1995).

[20] A. Splendiani, L. Sun, Y. Zhang, T. Li, J. Kim, C. Y. Chim, G. Galli, and F. Wang, *Emerging Photoluminescence in Monolayer* MoS_2, Nano Lett. **10**, 1271 (2010).

[21] K. F. Mak, C. Lee, J. Hone, J. Shan, and T. F. Heinz, *Atomically Thin* MoS_2*: A New Direct-Gap Semiconductor*, Phys. Rev. Lett. **105**, 136805 (2010).

[22] T. Cheiwchanchamnangij and W. R. L. Lambrecht, *Quasiparticle Band Structure Calculation of Monolayer, Bilayer, and Bulk* MoS_2, Phys. Rev. B **85**, 205302 (2012).

[23] X. Duan, C. Wang, A. Pan, R. Yu, and X. Duan, *Two-Dimensional Transition Metal Dichalcogenides as Atomically Thin Semiconductors: Opportunities and Challenges*, Chem. Soc. Rev. **44**, 8859 (2015).

[24] X. Li, F. Zhang, and Q. Niu, *Unconventional Quantum Hall Effect and Tunable Spin Hall Effect in Dirac Materials: Application to an Isolated* MoS_2 *Trilayer*, Phys. Rev. Lett. **110**, 066803 (2013).

[25] F. Rose, M. O. Goerbig, and F. Piéchon, *Spin- and Valley-Dependent Magneto-Optical Properties of* MoS_2, Phys. Rev. B **88**, 125438 (2013).

[26] T. Cai, S. A. Yang, X. Li, F. Zhang, J. Shi, W. Yao, and Q. Niu, *Magnetic Control of the Valley Degree of Freedom of Massive Dirac Fermions with Application to Transition Metal Dichalcogenides*, Phys. Rev. B **88**, 115140 (2013).

[27] X. Xu, W. Yao, D. Xiao, and T. F. Heinz, *Spin and Pseudospins in Layered Transition Metal Dichalcogenides*, Nat. Phys. **10**, 343 (2014).

[28] D. Xiao, W. Yao, and Q. Niu, *Valley-Contrasting Physics in Graphene: Magnetic Moment and Topological Transport*, Phys. Rev. Lett. **99**, 236809 (2007).

[29] Z. Wang, J. Shan, and K. F. Mak, *Valley- and Spin-Polarized Landau Levels in Monolayer* WSe_2, Nat. Nanotechnol. **12**, 144 (2017).

[30] T. Smoleński *et al.*, *Interaction-Induced Shubnikov–de Haas Oscillations in Optical Conductivity of Monolayer* $MoSe_2$, Phys. Rev. Lett. **123**, 097403 (2019).

[31] A. Chernikov, A. M. Van Der Zande, H. M. Hill, A. F. Rigosi, A. Velauthapillai, J. Hone, and T. F. Heinz, *Electrical Tuning of Exciton Binding Energies in Monolayer* WS_2, Phys. Rev. Lett. **115**, 126802 (2015).

[32] B. Zhu, X. Chen, and X. Cui, *Exciton Binding Energy of Monolayer* WS_2, Sci. Rep. **5**, 9218 (2015).

[33] C. Zhang, H. Wang, W. Chan, C. Manolatou, and F. Rana, *Absorption of Light by Excitons and Trions in Monolayers of Metal Dichalcogenide* MoS_2*: Experiments and Theory*, Phys. Rev. B **89**, 205436 (2014).

[34] K. F. Mak, K. He, C. Lee, G. H. Lee, J. Hone, T. F. Heinz, and J. Shan, *Tightly Bound Trions in Monolayer* MoS_2, Nat. Mater. **12**, 207 (2013).

[35] J. S. Ross *et al.*, *Electrical Control of Neutral and Charged Excitons in a Monolayer Semiconductor*, Nat. Commun. **4**, 1474 (2013).

[36] D. K. Efimkin and A. H. MacDonald, *Many-Body Theory of Trion Absorption Features in Two-Dimensional Semiconductors*, Phys. Rev. B **95**, 035417 (2017).

[37] D. K. Efimkin and A. H. MacDonald, *Exciton-Polarons in Doped Semiconductors in a Strong Magnetic Field*, Phys. Rev. B **97**, 235432 (2018).

[38] Z. Li *et al.*, *Revealing the Biexciton and Trion-Exciton Complexes in BN Encapsulated* WSe_2, Nat. Commun. **9**, 3719 (2018).

[39] Z. Li *et al.*, *Emerging Photoluminescence from the Dark-Exciton Phonon Replica in Monolayer* WSe_2, Nat. Commun. **10**, 2469 (2019).

[40] Z. Li *et al.*, *Direct Observation of Gate-Tunable Dark Trions in Monolayer* WSe_2, Nano Lett. **19**, 6886 (2019).

[41] A. V. Stier, N. P. Wilson, K. A. Velizhanin, J. Kono, X. Xu, and S. A. Crooker, *Magnetooptics of Exciton Rydberg States in a Monolayer Semiconductor*, Phys. Rev. Lett. **120**, 057405 (2018).

[42] S. Y. Chen *et al.*, *Luminescent Emission of Excited Rydberg Excitons from Monolayer* WSe_2, Nano Lett. **19**, 2464 (2019).

[43] M. Goryca *et al.*, *Revealing Exciton Masses and Dielectric Properties of Monolayer Semiconductors with High Magnetic Fields*, Nat. Commun. **10**, 4172 (2019).

[44] M. Manca *et al.*, *Enabling Valley Selective Exciton Scattering in Monolayer* WSe_2 *through Upconversion*, Nat. Commun. **8**, 14927 (2017).

[45] M. R. Molas, A. O. Slobodeniuk, K. Nogajewski, M. Bartos, Ł. Bala, A. Babiński, K. Watanabe, T. Taniguchi, C. Faugeras, and M. Potemski, *Energy Spectrum of Two-Dimensional Excitons in a Nonuniform Dielectric Medium*, Phys. Rev. Lett. **123**, 136801 (2019).

[46] S. Y. Chen, T. Goldstein, J. Tong, T. Taniguchi, K. Watanabe, and J. Yan, *Superior Valley Polarization and Coherence of* $2s$ *Excitons in Monolayer* WSe_2, Phys. Rev. Lett. **120**, 046402 (2018).

[47] D. Van Tuan, B. Scharf, I. Žutić, and H. Dery, *Marrying Excitons and Plasmons in Monolayer Transition-Metal Dichalcogenides*, Phys. Rev. X **7**, 041040 (2017).

[48] D. Xiao, G.-B. Liu, W. Feng, X. Xu, and W. Yao, *Coupled Spin and Valley Physics in Monolayers of* MoS_2 *and Other Group-VI Dichalcogenides*, Phys. Rev. Lett. **108**, 196802 (2012).

[49] G.-B. Liu, W. Y. Shan, Y. Yao, W. Yao, and D. Xiao, *Three-Band Tight-Binding Model for Monolayers of Group-VIB Transition Metal Dichalcogenides*, Phys. Rev. B **88**, 085433 (2013).

[50] K. He, N. Kumar, L. Zhao, Z. Wang, K. F. Mak, H. Zhao, and J. Shan, *Tightly Bound Excitons in Monolayer* WSe_2, Phys. Rev. Lett. **113**, 026803 (2014).

[51] A. Chernikov, T. C. Berkelbach, H. M. Hill, A. Rigosi, Y. Li, O. B. Aslan, D. R. Reichman, M. S. Hybertsen, and T. F. Heinz, *Exciton Binding Energy and Nonhydrogenic Rydberg Series in Monolayer* WS_2, Phys. Rev. Lett. **113**, 076802 (2014).

[52] See the Supplemental Material at http://link.aps.org/supplemental/10.1103/PhysRevX.10.021024 for details of experimental methods, theoretical modeling, and supplemental figures.

[53] V. P. Gusynin, S. G. Sharapov, and J. P. Carbotte, *Anomalous Absorption Line in the Magneto-Optical Response of Graphene*, Phys. Rev. Lett. **98**, 157402 (2007).

[54] Y. P. Shkolnikov, E. P. De Poortere, E. Tutuc, and M. Shayegan, *Valley Splitting of AlAs Two-Dimensional Electrons in a Perpendicular Magnetic Field*, Phys. Rev. Lett. **89**, 226805 (2002).

[55] W. Chen, M. Fritze, A. V. Nurmikko, D. Ackley, C. Colvard, and H. Lee, *Interaction of Magnetoexcitons and Two-Dimensional Electron Gas in the Quantum Hall Regime*, Phys. Rev. Lett. **64**, 2434 (1990).

[56] B. B. Goldberg, D. Heiman, A. Pinczuk, L. Pfeiffer, and K. West, *Optical Investigations of the Integer and Fractional Quantum Hall Effects: Energy Plateaus, Intensity Minima, and Line Splitting in Band-Gap Emission*, Phys. Rev. Lett. **65**, 641 (1990).

[57] B. M. Ashkinadze, E. Linder, E. Cohen, V. V. Rudenkov, P. C. M. Christianen, J. C. Maan, and L. N. Pfeiffer, *Exciton to Two-Dimensional Electron-Hole Photoluminescence Transitions Driven by the Quantum Hall Effect in Photoexcited Heterojunctions*, Phys. Rev. B **72**, 075332 (2005).

[58] A. Krakovsky and J. K. Percus, *Quasiparticle Effective Mass for the Two- and Three-Dimensional Electron Gas*, Phys. Rev. B **53**, 7352 (1996).

[59] A. Isihara and T. Toyoda, *Two-Dimensional Electron Gas at Finite Temperature*, Phys. Rev. B **21**, 3358 (1980).